BIOCHEMISTRY
including biophysical chemistry & molecular biology

Article

pubs.acs.org/biochemistry

Mechanistic Insights into Mg^{2+}-Independent Prenylation by CloQ from Classical Molecular Mechanics and Hybrid Quantum Mechanics/Molecular Mechanics Molecular Dynamics Simulations

Craig A. Bayse[†] and Kenneth M. Merz*[,‡,§]

[†]Department of Chemistry and Biochemistry, Old Dominion University, Norfolk, Virginia 23518, United States

[‡]Department of Chemistry and Quantum Theory Project, University of Florida, Gainesville, Florida 32611, United States

[§]Institute for Cyber Enabled Research, Department of Chemistry, and Department of Biochemistry and Molecular Biology, Michigan State University, East Lansing, Michigan 48824, United States

ABSTRACT: Understanding the mechanism of prenyltransferases is important to the design of engineered proteins capable of synthesizing derivatives of naturally occurring therapeutic agents. CloQ is a Mg^{2+}-independent aromatic prenyltransferase (APTase) that transfers a dimethylallyl group to 4-hydroxyphenylpyruvate in the biosynthetic pathway for clorobiocin. APTases consist of a common ABBA fold that defines a β-barrel containing the reaction cavity. Positively charged basic residues line the inside of the β-barrel of CloQ to activate the pyrophosphate leaving group to replace the function of the Mg^{2+} cofactor in other APTases. Classical molecular dynamics simulations of CloQ, its E281G and F68S mutants, and the related NovQ were used to explore the binding of the 4-hydroxyphenylpyruvate (4HPP) and dimethylallyl diphosphate substrates in the reactive cavity and the role of various conserved residues. Hybrid quantum mechanics/molecular mechanics potential of mean force (PMF) calculations show that the effect of the replacement of the Mg^{2+} cofactor with basic residues yields a similar activation barrier for prenylation to Mg^{2+}-dependent APTases like NphB. The topology of the binding pocket for 4HPP is important for selective prenylation at the ortho position of the ring. Methylation at this position alters the conformation of the substrate for O-prenylation at the phenol group. Further, a two-dimensional PMF scan shows that a "reverse" prenylation product may be a possible target for protein engineering.

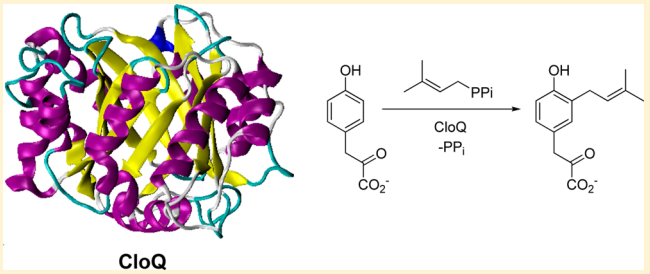

Aromatic prenyltransferases (APTases) catalyze the biological Friedel–Crafts-like alkylation of a variety of organic substrates.[1−6] These proteins activate the prenyl diphosphate carrier to release a carbocation that attacks an aromatic ring or other nucleophilic site on the substrate. Prenylation increases the affinity of molecules for cell walls through the addition of a hydrophobic group. These molecules have been shown to be effective antibiotics and antitumor agents but are difficult to synthesize and are present at concentrations too low for practical extraction from natural sources. Understanding the mechanisms of these enzymes is important for the engineering of proteins designed to synthesize related drugs and inhibitors.[7,8]

Early examples of membrane prenyltransferases were found to rely on Mg^{2+} for the activation of the pyrophosphate leaving group. These membrane PTases were characterized by an anionic (N/D)DxxD binding site for the Mg^{2+} ion. More recently, a new class of soluble PTases lacking this binding site and not necessarily dependent upon the Mg^{2+} cofactor have been identified. NphB, the first of these aromatic prenyltransferases (APTases), uses Mg^{2+} to transfer a geranyl group to various small organic substrates.[2] Mg^{2+}-independent APTases such as CloQ[9,10] and the dimethylallyl tryptophan synthase (DMATS)[11−13] family have also been identified. These enzymes replace Mg^{2+} with positively charged amino acid residues such as Arg and Lys to stabilize the release of the pyrophosphate leaving group. Although CloQ and DMATS are Mg^{2+}-free, they are not homologous, yet CloQ is 16% homologous to the Mg^{2+}-dependent NphB.

APTases have been grouped by sequence similarity into the CloQ/NphB and DMATS/CymD families. CloQ and the related NovQ catalyze the prenylation of 4-hydroxyphenylpyruvate (4HPP) by dimethylallyl diphosphate (DMAPP) along the biosynthetic pathway of the antibiotics clorobiocin and novobiocin (Figure 1).[9,10,14] Although CloQ appears to be specific to 4-HPP, NovQ (84% homologous) prenylates a broad range of phenylpropanoids and flavonoids, albeit with low yields.[14] Additional members of the CloQ/NphB family have been identified, including the phenazine APTases EpzP/PpzP,[8,15] the Mg^{2+}-dependent Fur7 that catalyzes the geranylization of various phenol and flavinoid substrates,[16] and the related Fnq26 that appears to be unique in that it is Mg^{2+}-independent and uses geranyl diphosphate (GPP).[17] In

Received: May 3, 2014
Revised: June 20, 2014
Published: July 14, 2014

   dx.doi.org/10.1021/bi500531p | *Biochemistry* 2014, 53, 5034−5041

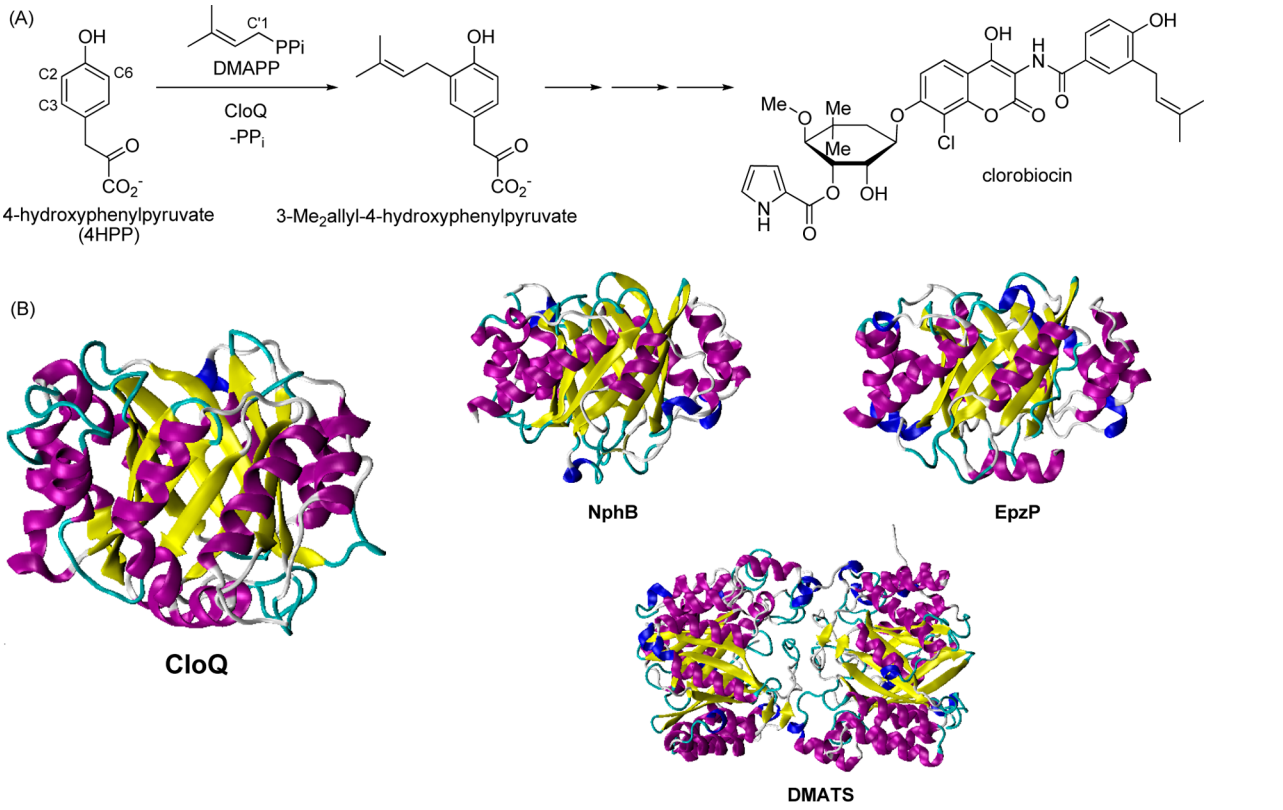

Figure 1. (A) Prenylation of 4HPP catalyzed by CloQ as part of the biosynthesis of clorobiocin. (B) Comparison of structures of proteins in the CloQ/NphB and DMATS families.

contrast, DMATS enzymes prenylate indoles at various positions for precursors along the biosynthetic pathway of LSD and other alkaloids.[18]

Structural information is available for several APTases of the CloQ/NphB family.[2,8−10] These proteins consist of five $\alpha\beta\beta\alpha$ domains forming a barrel of 10 antiparallel β-sheets that defines the reaction cavity. The β-barrel is surrounded by 10 solvent-accessible α-helices. These proteins conserve a number of residues that allow for binding of the prenylation carriers, but the residues that make up the reaction cavity vary to accommodate substrates of different sizes.[8] In cases in which crystal structures of substrate-bound proteins have been obtained, these residues have been identified and assigned specific roles in either substrate binding or specificity. In general, the reaction cavity contains two regions: a prenyl carrier binding and activation site and the substrate binding site. Unlike NphB and DMATS, the bottom of the barrel of CloQ, containing the 4HPP binding site, appears to be closed to form a hydrophobic pocket.

The prenylation mechanism has been the subject of much debate, especially for farnesyl transferases (FTases),[19] with an associative mechanism (S_N2-like), a dissociative mechanism (S_N1-like), and an associative mechanism with dissociative characteristics proposed.[2] Molecular modeling has played an important role in characterizing the mechanisms of PTases such as NphB[20] and in the related FTases.[21−23] In this paper, classical molecular mechanics (MM) and hybrid quantum mechanics/molecular mechanics (QM/MM) methods using the self-consistent charge density functional tight-binding (SCC-DFTB)[24−26] theory are used to model substrate binding and the prenylation mechanism of CloQ for comparison with those of the previously studied Mg^{2+}-dependent NphB.[20]

COMPUTATIONAL METHODS

MM and QM/MM MD simulations were performed using the sander and PMEMD routines in Amber 12.[27] The protein was represented by the *ff99sb* force field,[28] and the general atomic force field GAFF[29] was used for DMAPP and 4HPP. Parameters and BCC charges for 4HPP and DMAPP were obtained using ANTECHAMBER. Long-range interactions were modeled using the particle mesh Ewald method (cutoff of 8 Å).[30]

Classical and QM/MM MD Simulations of CloQ. The CloQ model was constructed using residues 7−313 of the protein from the crystal structure with the substrate 4HPP bound to the active site (Protein Data Bank entry 2XLQ).[10] H++[31] predicted four protonation sites of the apoprotein: His168 and His223 located at the mouth of the reaction cavity and His307 and His313 at the C-terminus. These residues were modeled using the HIP parameters for protonated histidine. The CloQ/4HPP/DMAPP system had an overall charge of −7, which was neutralized by sodium ions. Water molecules found in the crystal structure were retained, and an octahedral box of TIP3P[32] water was added to the system (12298 total waters). Bond lengths involving hydrogen were constrained using SHAKE unless otherwise noted. UCSF DOCK 6.6 was used to fit DMAPP into the reaction cavity, and the system was equilibrated to seat the substrate. After the system had been warmed and equilibrated at 300 K using Langevin dynamics in the *NVT* ensemble, the system was equilibrated in the *NPT* ensemble prior to a 120 ns production simulation (time step of 2 fs). Similar MD simulations of apo-CloQ, apo-NovQ, and the F68S and E281G mutants were performed to compare the stability of the substrates in the binding pocket.

dx.doi.org/10.1021/bi500531p | *Biochemistry* 2014, 53, 5034−5041

For the QM/MM simulations, the 4HPP and DMAPP substrates were modeled using the SCC-DFTB[24] method with the remainder of the system treated with the *ff99sb* force field. SCC-DFTB has been shown to be a reliable semiempirical method for enzymatic reactions, providing geometries and energetics comparable to those of B3LYP.[25] Moreover, we have utilized it in previous studies involving FTase[21−23] and NphB[20] with excellent success. The entire system was minimized for 1000 steps followed by heating to 300 K in the *NVT* ensemble (50 ps, time step of 0.5 fs) and equilibrated for 950 ps in the *NPT* ensemble to prepare the system for potential of mean force (PMF) calculations.

QM/MM Potential of Mean Force Calculations of Prenylation by CloQ. One-dimensional PMF curves were determined by steered MD (SMD) calculations of the trajectories along the C1′−O (D_{C-O}) and C1′−C2 (D_{C-C}) reaction coordinates with force constants of 150 and 250 kcal mol^{-1} Å^{-2}, respectively, for the biasing potentials. The two-dimensional (2D) PMF was constructed from umbrella sampling calculations of a grid of 750 windows over a D_{C-C} range of 1.4−4.0 Å and a D_{C-O} range of 1.4−4.1 Å. Windows were equilibrated for 75 ps at 300 K followed by data collection for 50 ps. Distances were saved every 10 fs. Unbiased distributions for one-dimensional (1D) and 2D PMFs were generated by the weighed histogram analysis method[33] (WHAM) using Grossfield's code[34] with statistical uncertainty estimated by Monte Carlo bootstrapping.

RESULTS AND DISCUSSION

Classical MD Simulations of Apo-CloQ and the CloQ/4HPP/DMAPP System. To model the Mg^{2+}-independent prenylation mechanism, a CloQ/4HPP/DMAPP complex was constructed from the X-ray structure of the CloQ/4HPP system using docking programs to fit DMAPP into the reaction cavity defined by the β-barrel. Equilibration of this CloQ/4HPP/DMAPP complex allowed the dimethylallyl group to move into a π-stacking position over the aromatic ring of 4HPP with close C1′−C2 and C3′−C6 contacts and intermolecular distances of 3.4−4.8 Å (Figure 2). Comparison of the backbone

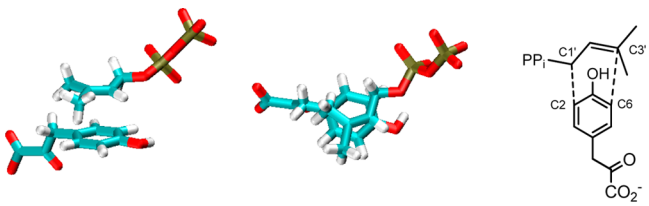

Figure 2. Schematic of the positioning of 4HPP and DMAPP in the CloQ active site. The distance between the dimethylallyl group and the phenyl ring ranges from 3.4 to 4.8 Å.

root-mean-square deviation (rmsd) and root-mean-square fluctuation (rmsf) for apo- and holo-CloQ (Figure 3) show that the overall structure of the protein does not change significantly upon binding of the substrates over the time scale of the simulation. The loop regions connecting the outer shell of α-helices are the most mobile, with the α8−α9 sequence being particularly active. Trp122 shows variable positioning in the X-ray structure,[10] but only one conformation is observed over the duration of the simulation of the apoprotein. For comparison, MD simulations were performed on a model of apo-NovQ created by point mutations of apo-CloQ [backbone rmsd = 1.7 (Figure 4)]. The nonhomologous residues, as determined by sequence alignment,[6] are located on the outer α-helices. Conserved residues, including those involved in substrate binding and activation, are oriented toward the interior of the β-barrel.

The reaction cavity is divided into two regions, a hydrophobic pocket that secures 4HPP at the bottom of the barrel and a highly positive portal that binds and activates DMAPP. Metzger et al. identified a series of residues lining the active site as having the role of stabilizing and/or activating the pyrophosphate leaving group (Figure 5).[10] MD simulations confirm that Lys54, Arg66, Lys120, and Lys279 form hydrogen bonding interactions or salt bridges to the pyrophosphate group. These residues contribute to the high positive charge in the reaction cavity as shown in the surface electrostatic potential of apo-CloQ generated by APBS[35] (Figure 6). The net positive charge of the portal residues also cancels the negative charge of DMAPP contributing to the activation of the leaving group. Arg229 and Tyr277 are found not to interact directly with DMAPP as suggested by Metzger et al. but may assist in drawing it into the cavity. Several basic residues (e.g., Arg116 and Arg167) located around the rim of the β-barrel could serve the same function. Tyr174 and Tyr233 stabilize binding of DMAPP through hydrogen bonds to the terminal oxygen of P1 and form a wall between the positive portal of the reaction cavity and the hydrophobic pocket similar to that shown for NphB.[20]

The walls of the hydrophobic pocket consist of Phe68, Trp122, Tyr174, Tyr233, Leu235, Phe161, Val166, Leu292, and Trp295. The residues that line the hydrophobic pocket help define its size to contribute to substrate selectivity. The reaction cavity positions DMAPP and 4HPP in the ideal position for rapid C−C bond formation. EpzP also has a well-defined binding pocket that restricts the reactivity of its substrate.[8] The pocket appears to have room to accommodate larger substrates such as flavonoids as shown for NovQ, where O-prenylated products are sometimes obtained in addition to prenylation of the aromatic ring.[14] The hydrophobic pocket has been proposed to protect the dimethylallyl cation from being quenched by water, but several waters are found close to 4HPP in the simulations and likely facilitate deprotonation of the arenium ion intermediate (also known as the Wheland intermediate[36]). Similarly, catalytic water molecules were identified in the X-ray structure of EpzP.[8]

Polar groups on either end of the hydrophobic pocket anchor 4HPP in position through interactions with the phenol (Glu281) and carboxylate groups (Arg160 and Arg176). The stabilizing effects of Arg176, not identified by Metzger et al. as an important residue, may contribute to the partial retention of activity of the R160A and R160Q mutants. Although the X-ray structure indicates the formation of a bond between Cys215 and 4HPP, these residues are treated as nonbonded in this study because the C215S and C215A mutants demonstrated similar, or improved, activity relative to that of the wild type (WT).[10] Cys215 and Cys297 appear to bookend the α-keto acid to stabilize 4HPP through electrostatic interactions between the thiols and the partially positive carbons of the pyruvate group (Figure 5). The importance of the anchoring residues Arg160, Arg176, and Glu281 may contribute to 4-hydroxybenzoic acid not being a substrate for CloQ because it is too small to bridge both sites. However, molecules like coumaric acid can be prenylated, but much more slowly

dx.doi.org/10.1021/bi500531p | *Biochemistry* 2014, 53, 5034−5041

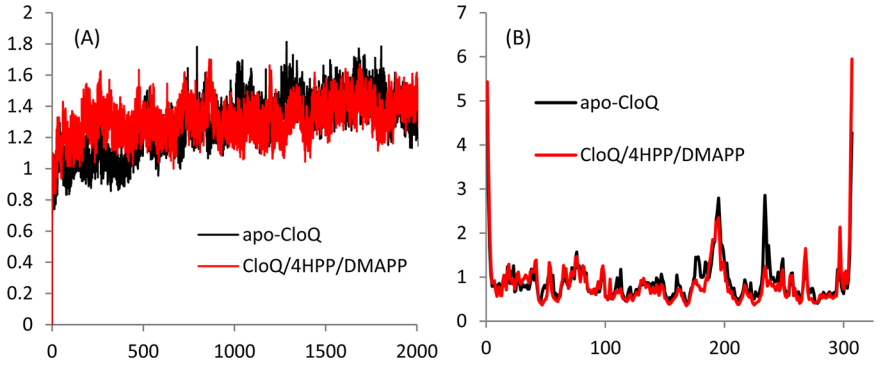

Figure 3. (A) rmsd and (B) rmsf of apo-CloQ (black) and the CloQ/4HPP/DPP complex (red).

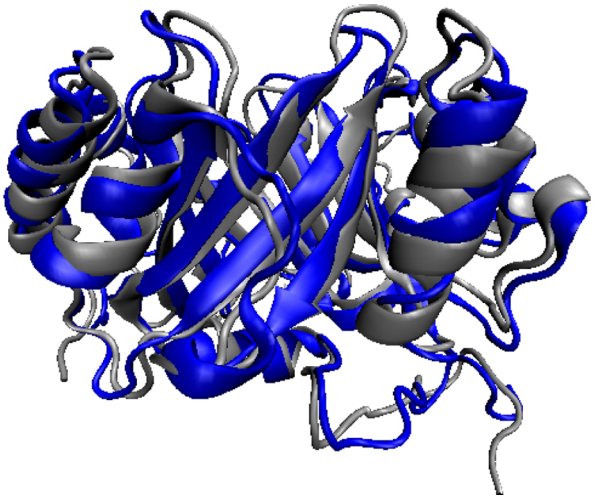

Figure 4. Overlay of the apo forms of CloQ (blue) and NovQ (silver).

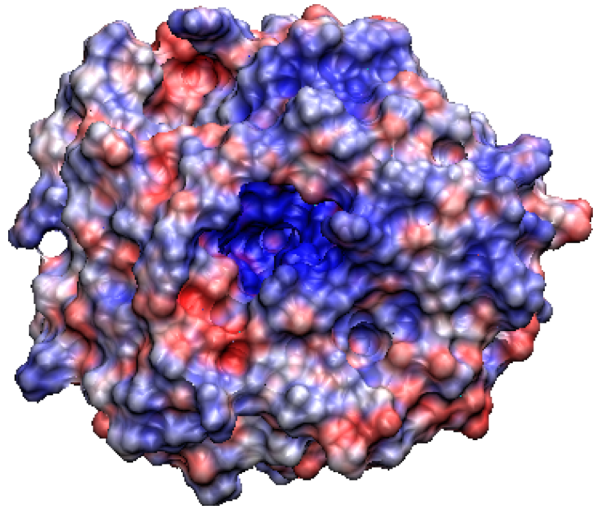

Figure 6. Electrostatic potential of apo-CloQ.

because the binding in the pocket may not be stabilized by electrostatic interactions with Cys215 and Cys297.

MD studies of the E281G and F68S mutants suggest that their reduced activity (1 and 6.2% of that of WT, respectively)

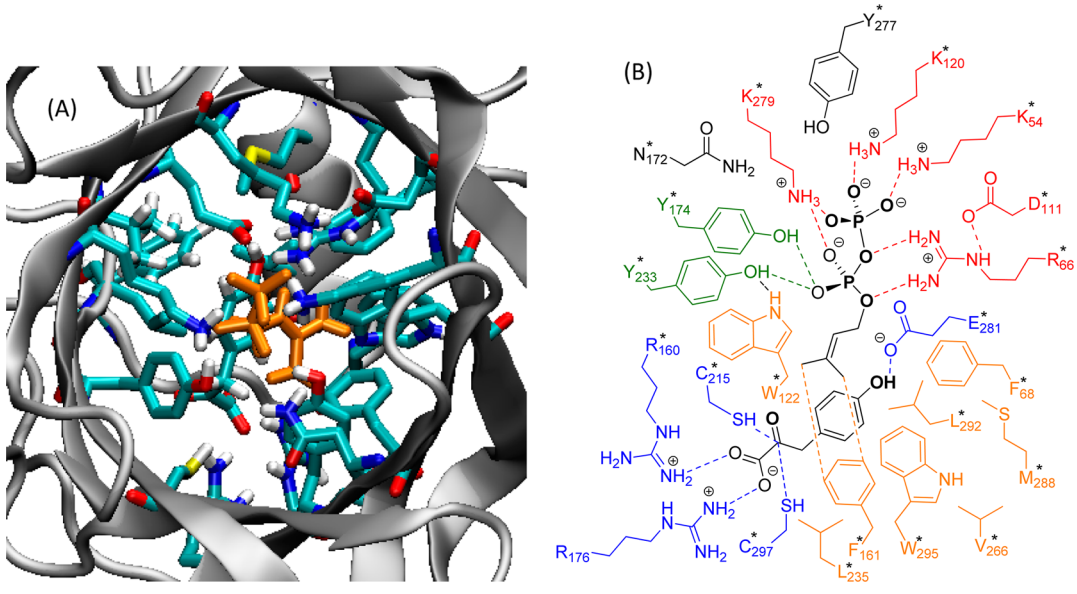

Figure 5. Schematic of the interactions of 4HPP and DMAPP in the CloQ binding site. (A) View down the barrel showing the interactions between basic residues and DMAPP (orange). (B) Diagram of the interactions of 4HPP and DMAPP with the residues that make up the reaction cavity. Residues colored red interact with DMAPP in the positive portal. The Tyr shield is colored green, and the anchor residues are colored blue and the walls of the hydrophobic pocket orange. The residues marked with asterisks were proposed by Metzger et al. to interact with DMAPP and 4HPP.

dx.doi.org/10.1021/bi500531p | *Biochemistry* 2014, 53, 5034−5041

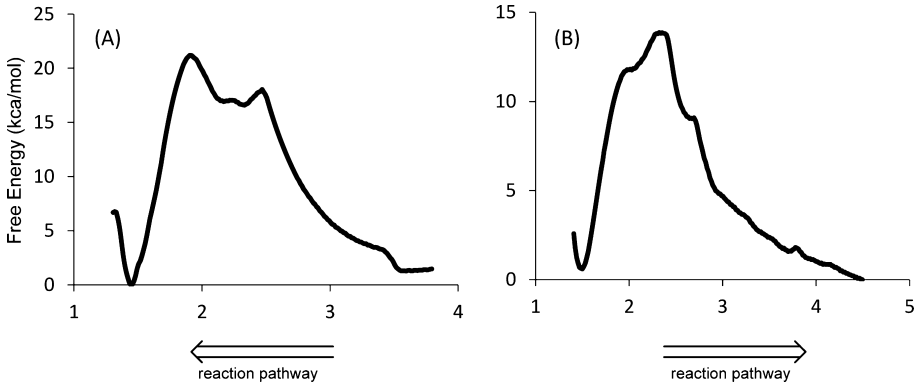

Figure 7. 1D PMFs for (A) C1′−C2 bond formation and (B) C1′−O bond breaking pathways.

can be attributed to the loss of definition of the binding pocket. The loss of the hydrogen bond or salt bridge between E281 and the 4HPP phenol was expected to primarily affect the positioning of 4HPP in the hydrophobic pocket.[10] However, the MD simulation shows that the pocket keeps 4HPP largely in place in the E281 mutant but allows DMAPP to settle deeper into the hydrophobic pocket such that the dimethylallyl group is no longer sandwiched between Trp122 and 4HPP. Therefore, the E281−4HPP interaction limits the size of the prenylating agent to favor DMAPP over larger substrates.[2] Fnq26 and NphB, which use the larger GPP, replace Asp with Gly. Phe68 was proposed to restrict the size of the prenyl binding pocket relative to that of NphB, which uses the larger GPP as a substrate. In MD simulations of F68S, the mutation appears to destabilize the binding of DMAPP, which undergoes changes in conformation several times during the simulation.

Metzger et al. used Tyr as a model of the keto form of DMAPP but found a decrease in activity of 2 orders of magnitude.[10] In MD simulations of the CloQ/Tyr/DMAPP system, Tyr was inserted into the binding site with the carboxylate deprotonated and the amine neutral in analogy to the protonation state of 4HPP in the MD models. MD simulations show that the Tyr substrate is less stably bound to the hydrophobic pocket. The lack of similarity between the electrostatics of the -$CHNH_2$ group and the partial positive charge of the carbon end of the carbonyl does not allow for the amino acid to be sandwiched between Cys215 and Cys297. These residues prefer to hydrogen bond to the Tyr carboxylate group leading to a small shift toward Glu281, which misaligns Tyr with DMAPP in the hydrophobic pocket.

QM/MM MD Simulation and PMF Study of the CloQ-Catalyzed Prenylation of DMAPP. Steered MD scans were performed from the CloQ/4HPP/DMAPP complex to the Wheland intermediate[36] by following both the C1′−C2 bond formation and C1′−O bond breaking coordinates. C1′−C2 bond formation led to a dissociative pathway for prenylation in which the C1′−O bond of DMAPP first cleaves to form the dimethylallyl cation (DMA^+) followed by C1′−C2 bond formation (Figures 7A and 8A). 4HPP, Trp122, and other residues form a "π-chamber" around the DMA^+ intermediate similar to that found in simulations of prenylation by NphB.[20] Cation−π interactions between the aromatic residues of the hydrophobic pocket stabilize and position DMA^+ over 4HPP for selective C1′−C2 bond formation. Alternate SMD scans to force C1′−C3 bond formation lead instead to the C1′−C2 bond through a cation−π intermediate. This result is consistent with C2 being the natural target for prenylation in DMAPP.

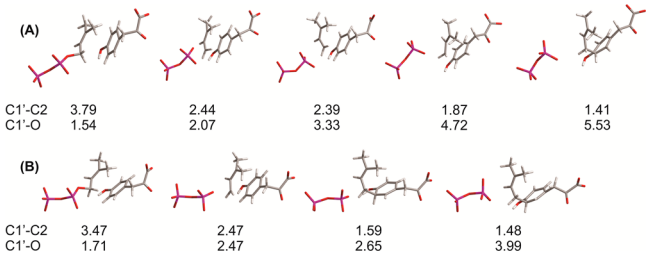

Figure 8. Snapshots of the prenylation of 4HPP along the (A) C1′−C2 bond formation and (B) C1′−O bond breaking pathways. Distances are in angstroms.

Mulliken charges verify that C2/C6 is the most electrophilic position on the phenyl ring as expected for the para arrangement of an ortho and meta director.

A different profile is obtained along the C−O bond breaking PMF (Figures 7B and 8B). Here, no distinct intermediate is observed, and the process appears to be generally associative, with C1′−C2 bond formation appearing to be concurrent with C1′−O bond cleavage. Interestingly, the transition state for C1′−O bond breakage along this pathway is lower than that of C−C bond formation (~13 kcal/mol vs ~20 kcal/mol). The higher barrier for the latter is typical for SMD of bond formation pathways in which repulsive interactions must be overcome.[37] In each PMF, the pyrophosphate leaving group drifts back into the portal to strengthen its interactions with the basic residues.

Because inconsistent results were obtained along the 1D reaction coordinates, a 2D PMF was constructed with respect to the C1′−C2 and C1′−O coordinates (Figure 9). The 4HPP/DMAPP reactant lies in a broad well around a C1′−C2 distance of 3.5 Å. The Wheland intermediate is separated from the reactant well by a ridge approximately 13−15 kcal/mol high, comparable to the activation barriers for prenylation by the Mg^{2+}-dependent NphB.[20] A shallow valley for the cation−π intermediate runs parallel to the product basin, separated by a small barrier. From the 2D PMF, the major process is primarily C1′−O bond cleavage, which is stabilized by the interactions between the basic groups and the pyrophosphate leaving group in the portal of the reaction cavity. As shown for NphB, the Wheland complex is ~4 kcal/mol more stable than the reactants.

Interestingly, a second shallow well is found at long C1′−C2 and C1′−O distances that is consistent with "reverse" prenylation at the far C2 site of 4HPP. Reverse prenylation by DMAPP, formation of a bond to C3′ rather than C1′, is

dx.doi.org/10.1021/bi500531p | Biochemistry 2014, 53, 5034−5041

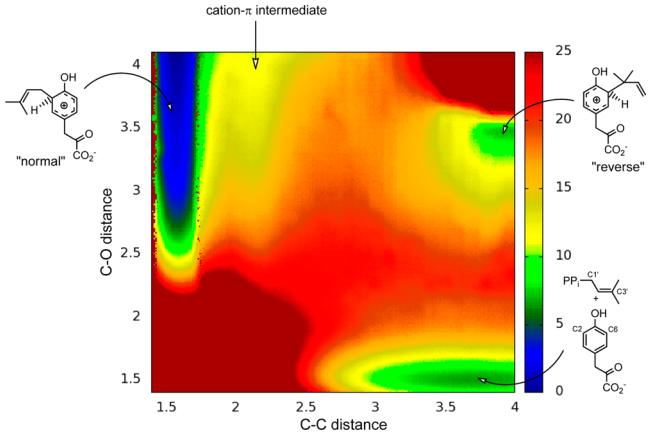

Figure 9. 2D PMF of the formation of the Wheland intermediate by prenylation at C2 of 4HPP. Note the shallow well for "reverse" prenylation at the far ortho position of 4HPP in the top right corner.

common in the DMATS family and has been reported for the Fur7 and Fnq26 members of the CloQ family.[16,17] A minor reverse prenylation product of 1,6-dihydroxynaphthalene was also observed with NovQ.[14] The barrier into this well is comparable to the primary pathway, suggesting that passage across the barrier to the major product may be correlated with cleavage of the C−O bond. The reverse product was not observed in any of the SMD runs, even though its barrier appears to be similar to the normal pathway. Steric interations between the methyl groups of DMAPP and the walls of the hydrophobic pocket may also discourage reaction via this pathway. Alternatively, the low barrier from the reverse to normal arenium ion may allow any reverse product to rapidly rearrange to the normal. In an attempt to access this product, simulations of prenylation of 3-Me-4HPP were performed. Two binding conformations of 3-Me-4HPP were equilibrated using classical MD simulations with the methyl group at either C2 (closest to C1′) or C6 (closest to C3′ and facing the outer wall of the hydrophobic pocket). These positions are technically equivalent but represent sites of normal and reverse prenylation for the CloQ-bound substrate. Both simulations prefer to orient the methyl group in the C6 position, and SMD runs along the C1′−O bond breaking coordinate led to O-prenylation at the phenol rather than C1′−C2 or C3′−C6 bond formation. The steric interactions of the additional methyl group prevent the substrate from properly aligning with DMAPP in the hydrophobic pocket (Figure 10). The barrier for O-prenylation (18.7 kcal/mol) is comparable to that for C-prenylation (13.9 kcal/mol) and may lead to competition between these pathways depending upon the orientation of the substrate in the hydrophobic pocket. For example, NovQ was shown to O-prenylate a number of large substrates, including *p*-coumaric acid, caffeic acid, and the flavonoids naringenin and genistein.[14] Whereas O-prenylation is the major product for *p*-coumaric acid (34.4% vs 16.8%), C-prenylation is dominant for naringenin (11.1% vs 87.2%). The reduced rate and the loss of specificity for these cases could be attributed to the improper positioning of these substrates. It is not clear, given the size of the hydrophobic pocket for CloQ and NovQ, how larger molecules such as flavonoids can be prenylated. The bottom of the reactive cavity of CloQ and NovQ appears to be closed by helix η7, but the Arg anchors for 4HPP lie at the edge of a possible cleft that may serve as the entrance to the hydrophobic pocket. A larger substrate may be able to protrude through this

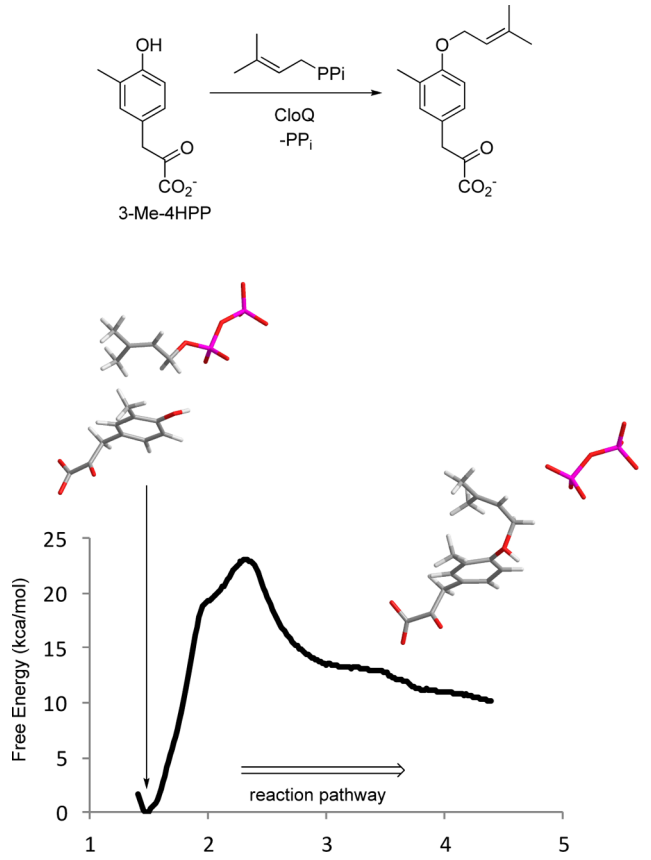

Figure 10. 1D PMF for the C1′−O bond breaking pathway shows O-prenylation of the phenol.

cleft. Like the open end of the positive portal, several basic groups are close to this cleft and could serve to guide substrates into the bottom of the pocket.

Deprotonation of the Wheland-type intermediate restores aromaticity to the ring but is not expected to be rate-determining because of the driving force for this rearrangement. A potential role in this process for Asp281 was proposed by Metzger et al.,[10] but the hydrogen bonding interaction between its carboxylate and the 4HPP phenol keeps this residue too far removed from the deprotonation site. X-ray studies of the CloQ/4HPP complex did not report water molecules in the hydrophobic pocket, but several leak into the reaction cavity during the simulation either through the portal or through a small gap at the bottom of the barrel. Deprotonation by an active site water has also been proposed for EpzP[8] and NphB.[20] PMF studies of NphB yield activation barriers for deprotonation by water of ∼7.7 kcal/mol, which was significantly lower than the barrier for transfer to a much more distant Tyr residue.[20]

QM/MM MD simulations of the deprotonation step used an expanded QM region to include the side chain of Arg281 and several active site waters in the proximity of the target proton. With SHAKE turned off, deprotonation is spontaneous to the nearest water molecule during the equilibration runs, which indicates that there is effectively no barrier to this process. Extended simulations of the system after deprotonation suggest that the hydronium ion may prefer to associate with the more negatively charged pyrophosphate over the Asp carboxylate. This conclusion would be consistent with the retention of some activity in the E281A mutant and its principle role in the

dx.doi.org/10.1021/bi500531p | *Biochemistry* 2014, 53, 5034−5041

positioning of the 4HPP and DMAPP substrates. The protonation of the pyrophosphate may also facilitate its exit from the reaction cavity.

Comparison to NphB. The related APTase NphB transfers a geranyl group to a number of substrates but, unlike CloQ, requires a Mg^{2+} ion to catalyze the reaction. Early reports suggested that Mg^{2+} has a slight effect on CloQ,[9] but later studies demonstrated that prenylation does not require the assistance of the ion cofactor. QM/MM studies of NphB suggested that the reaction proceeds by an S_N1-type pathway and that the cation−π interactions within the reaction cavity stabilize the formation of the carbocation. Other APTases use similar features to activate the carbocation: FtmPt1 employs a "tyrosine shield" allowing for experimental evidence of a short-lived DMA^+ intermediate.[7] Effectively, these Tyr residues act as a fulcrum to separate the pyrophosphate leaving group from the carbocation. In contrast, CloQ may be best characterized as associative with dissociative characteristics because of the tight packing of 4HPP and DMAPP substrates with C1′ and C2 positioned for immediate bond formation. However, prenylation of other substrates, such as those shown for NovQ, may follow a more dissociative pathway because of imperfect binding to the hydrophobic pocket. The mechanisms of CloQ, NphB, and other APTases are in contrast to those of the FTases that catalyze the S_N2-like prenylation of the sulfur of a Cys residue.[19]

CONCLUSIONS

Mg^{2+}-independent APTases employ basic residues to activate the pyrophosphate leaving group. QM/MM PMF calculations of the prenylation mechanism of CloQ show that the effect of these residues is similar to that of the Mg^{2+} cofactor in the related NphB. The high selectivity of CloQ can be attributed to the size of the reactive cavity and the directing properties of the ring substituents of the 4HPP substrate. Classical MD simulations of the protein docked with DMAPP show that the reactive cavity positions the prenylating group into the ideal position for selective transfer to C2 of 4HPP. The MD simulations clarify the roles of several residues in the reactive cavity. Electrostatic interactions between residues Cys215 and Cys297 and the pyruvate group of 4HPP limit substrate motion in the hydrophobic pocket. Glu281 also helps position 4HPP through a salt bridge or hydrogen bond to the phenol group to block DMAPP from working its way into the pocket, enforcing selectivity for both DMAPP and 4HPP. The definition of the hydrophobic pocket appears to be the key to the specificity for the transfer of a prenyl group to the ring, and point mutations of the residues that define the pocket may be a target for protein engineering. Simulations of 3-Me-4HPP predict O-prenylation of the phenol as observed for flavonoids with the related NovQ, suggesting that bulky groups misalign the substrate in the hydrophobic pocket. The study also shows that a reverse prenylation product, common to DMATS-catalyzed prenylation, may be accessible by careful modification of the residues of the hydrophobic pocket.

AUTHOR INFORMATION

Corresponding Author

*E-mail: kmerz1@gmail.com.

Notes

The authors declare no competing financial interest.

ACKNOWLEDGMENTS

C.A.B. thanks K.M.M. for hosting a sabbatical appointment at the University of Florida and Dhruva Chakravorty and Li-Li Pan for helpful discussions.

REFERENCES

(1) Liang, P.-H., Ko, T.-P., and Wang, A. H.-J. (2002) Structure, Mechanism and Function of Prenyltransferases. *Eur. J. Biochem. 269*, 3339−3354.

(2) Kuzuyama, T., Noel, J. P., and Richard, S. B. (2005) Structural Basis for the Promiscuous Biosynthetic Prenylation of Aromatic Natural Products. *Nature 435*, 983−987.

(3) Tello, M., Kuzuyama, T., Heide, L., Noel, J. P., and Richard, S. B. (2008) The ABBA Family of Aromatic Prenyltransferases: Broadening Natural Product Diversity. *Cell. Mol. Life Sci. 65*, 1459−1463.

(4) Heide, L. (2009) Prenyl Transfer to Aromatic Substrates: Genetics and Enzymology. *Curr. Opin. Chem. Biol. 13*, 171−179.

(5) Saleh, O., Haagen, Y., Seeger, K., and Heide, L. (2009) Prenyl Transfer to Aromatic Substrates in the Biosynthesis of Aminocoumarins, Meroterpenoids and Phenazines: The ABBA Prenyltransferase Family. *Phytochemistry 70*, 1728−1738.

(6) Bonitz, T., Alva, V., Saleh, O., Lupas, A. N., and Heide, L. (2011) Evolutionary Relationships of Microbial Aromatic Prenyltransferases. *PLoS One 6*, e27336.

(7) Jost, M., Zocher, G., Tarcz, S., Matuschek, M., Xie, X., Li, S.-M., and Stehle, T. (2010) Structure−Function Analysis of an Enzymatic Prenyl Transfer Reaction Identifies a Reaction Chamber with Modifiable Specificity. *J. Am. Chem. Soc. 132*, 17849−17858.

(8) Zocher, G., Saleh, O., Heim, J. B., Herbst, D. A., Heide, L., and Stehle, T. (2012) Structure-Based Engineering Increased the Catalytic Turnover Rate of a Novel Phenazine Prenyltransferase. *PLoS One 7*, e48427.

(9) Pojer, F., Wemakor, E., Kammerer, B., Chen, H., Walsh, C. T., Li, S.-M., and Heide, L. (2003) CloQ, a Prenyltransferase Involved in Clorobiocin Biosynthesis. *Proc. Natl. Acad. Sci. U.S.A. 100*, 2316−2321.

(10) Metzger, U., Keller, S., Stevenson, C. E. M., Heide, L., and Lawson, D. M. (2010) Structure and Mechanism of the Magnesium-Independent Aromatic Prenyltransferase CloQ from the Clorobiocin Biosynthetic Pathway. *J. Mol. Biol. 404*, 611−626.

(11) Edwards, D. J., and Gerwick, W. H. (2004) Lyngbyatoxin Biosynthesis: Sequence of Biosynthetic Gene Cluster and Identification of a Novel Aromatic Prenyltransferase. *J. Am. Chem. Soc. 126*, 11432−11433.

(12) Steffan, N., Unsöld, I. A., and Li, S.-M. (2007) Chemoenzymatic Synthesis of Prenylated Indole Derivatives by Using a 4-Dimethylallyltryptophan Synthase from *Aspergillus fumigatus*. *ChemBioChem 8*, 1298−1307.

(13) Schultz, A. W., Lewis, C. A., Luzung, M. R., Baran, P. S., and Moore, B. S. (2010) Functional Characterization of the Cyclomarin/Cyclomarazine Prenyltransferase CymD Directs the Biosynthesis of Unnatural Cyclic Peptides. *J. Nat. Prod. 73*, 373−377.

(14) Ozaki, T., Mishima, S., Nishiyama, M., and Kuzuyama, T. (2009) NovQ Is a Prenyltransferase Capable of Catalyzing the Addition of a Dimethylallyl Group to Both Phenylpropanoids and Flavonoids. *J. Antibiot. 62*, 385−392.

(15) Saleh, O., Gust, B., Boll, B., Fiedler, H.-P., and Heide, L. (2009) Aromatic Prenylation in Phenazine Biosynthesis: Dihydrophenazine-1-Carboxylate Dimethylallyltransferase from *Streptomyces anulatus*. *J. Biol. Chem. 284*, 14439−14447.

(16) Kumano, T., Tomita, T., Nishiyama, M., and Kuzuyama, T. (2010) Functional Characterization of the Promiscuous Prenyltransferase Responsible for Furaquinocin Biosynthesis Identification of a Physiological Polyketide Substrate and Its Prenylated Reaction Products. *J. Biol. Chem. 285*, 39663−39671.

(17) Haagen, Y., Unsöld, I., Westrich, L., Gust, B., Richard, S. B., Noel, J. P., and Heide, L. (2007) A Soluble, Magnesium-Independent Prenyltransferase Catalyzes Reverse and Regular C-Prenylations and O-Prenylations of Aromatic Substrates. *FEBS Lett. 581*, 2889−2893.

(18) Li, S.-M. (2010) Prenylated Indole Derivatives from Fungi: Structure Diversity, Biological Activities, Biosynthesis and Chemoenzymatic Synthesis. *Nat. Prod. Rep. 27*, 57−78.
(19) Huang, C., Hightower, K. E., and Fierke, C. A. (2000) Mechanistic Studies of Rat Protein Farnesyltransferase Indicate an Associative Transition State. *Biochemistry 39*, 2593−2602.
(20) Yang, Y., Miao, Y., Wang, B., Cui, G., and Merz, K. M. (2012) Catalytic Mechanism of Aromatic Prenylation by NphB. *Biochemistry 51*, 2606−2618.
(21) Cui, G., Wang, B., and Merz, K. M. (2005) Computational Studies of the Farnesyltransferase Ternary Complex Part I: Substrate Binding. *Biochemistry 44*, 16513−16523.
(22) Cui, G., and Merz, K. M. (2007) Computational Studies of the Farnesyltransferase Ternary Complex Part II: The Conformational Activation of Farnesyldiphosphate. *Biochemistry 46*, 12375−12381.
(23) Yang, Y., Wang, B., Ucisik, M. N., Cui, G., Fierke, C. A., and Merz, K. M. (2012) Insights into the Mechanistic Dichotomy of the Protein Farnesyltransferase Peptide Substrates CVIM and CVLS. *J. Am. Chem. Soc. 134*, 820−823.
(24) Elstner, M., Porezag, D., Jungnickel, G., Elsner, J., Haugk, M., Frauenheim, T., Suhai, S., and Seifert, G. (1998) Self-Consistent-Charge Density-Functional Tight-Binding Method for Simulations of Complex Materials Properties. *Phys. Rev. B 58*, 7260−7268.
(25) Cui, Q., Elstner, M., Kaxiras, E., Frauenheim, T., and Karplus, M. (2001) A QM/MM Implementation of the Self-Consistent Charge Density Functional Tight Binding (SCC-DFTB) Method. *J. Phys. Chem. B 105*, 569−585.
(26) Seabra, G. d. M., Walker, R. C., Elstner, M., Case, D. A., and Roitberg, A. E. (2007) Implementation of the SCC-DFTB Method for Hybrid QM/MM Simulations within the Amber Molecular Dynamics Package. *J. Phys. Chem. A 111*, 5655−5664.
(27) *AMBER 12* (2012) University of California, San Francisco.
(28) Hornak, V., Abel, R., Okur, A., Strockbine, B., Roitberg, A., and Simmerling, C. (2006) Comparison of Multiple Amber Force Fields and Development of Improved Protein Backbone Parameters. *Proteins: Struct., Funct., Bioinf. 65*, 712−725.
(29) Wang, J., Wolf, R. M., Caldwell, J. W., Kollman, P. A., and Case, D. A. (2004) Development and Testing of a General Amber Force Field. *J. Comput. Chem. 25*, 1157−1174.
(30) Darden, T., York, D., and Pedersen, L. (1993) Particle Mesh Ewald: An N log(N) Method for Ewald Sums in Large Systems. *J. Chem. Phys. 98*, 10089−10092.
(31) Anandakrishnan, R., Aguilar, B., and Onufriev, A. V. (2012) H++ 3.0: Automating pK Prediction and the Preparation of Biomolecular Structures for Atomistic Molecular Modeling and Simulations. *Nucleic Acids Res. 40*, W537−W541.
(32) Jorgensen, W. L., Chandrasekhar, J., Madura, J. D., Impey, R. W., and Klein, M. L. (1983) Comparison of Simple Potential Functions for Simulating Liquid Water. *J. Chem. Phys. 79*, 926−935.
(33) Kumar, S., Rosenberg, J. M., Bouzida, D., Swendsen, R. H., and Kollman, P. A. (1995) Multidimensional Free-Energy Calculations Using the Weighted Histogram Analysis Method. *J. Comput. Chem. 16*, 1339−1350.
(34) Grossfield, A. (2010) *WHAM: The weighted histogram analysis method*, University of Rochester Medical Center, Rochester, NY.
(35) Baker, N. A., Sept, D., Joseph, S., Holst, M. J., and McCammon, J. A. (2001) Electrostatics of Nanosystems: Application to Microtubules and the Ribosome. *Proc. Natl. Acad. Sci. U.S.A. 98*, 10037−10041.
(36) Wheland, G. W. (1942) A Quantum Mechanical Investigation of the Orientation of Substituents in Aromatic Molecules. *J. Am. Chem. Soc. 64*, 900−908.
(37) Ho, M.-H., Vivo, M. D., Peraro, M. D., and Klein, M. L. (2009) Unraveling the Catalytic Pathway of Metalloenzyme Farnesyltransferase through QM/MM Computation. *J. Chem. Theory Comput. 5*, 1657−1666.